

SaTor: Exploring Satellite Routing in Tor to Reduce Latency

Haozhi Li*

Beijing Institute of Technology
lihaozhi@bit.edu.cn

Tariq Elahi

University of Edinburgh
t.elahi@ed.ac.uk

Abstract—High latency is a critical limitation within the Tor network that has a negative impact on Web application responsiveness. A key factor exacerbating Tor latency is the creation of lengthy circuits that span across geographically distant regions, causing significant transmission delays. A common solution involves modifying Tor’s circuit-building process to reduce the likelihood of selecting lengthy circuits. However, this strategy compromises Tor’s routing randomness, increasing the risk of deanonymization. Reducing Tor’s latency while minimizing security degradation presents a challenge.

This paper proposes and investigates SaTor, a satellite-assisted routing scheme to reduce Tor latency. By equipping Tor relays with satellite network access, SaTor could accelerate slow circuits via satellite transmission, without biasing the existing path selection process. Our performance evaluation, using a simulator we developed along with real-world measurements, shows that over the long term, SaTor provides an expected speed-up of 21.8 ms for over 40% of circuits, with only 100 top relays equipped with satellite service. Our research uncovers a viable way to overcome Tor’s latency bottleneck, serving as a practical reference for its future enhancement.

1. Introduction

Tor is a popular tool for anonymous communication, protecting millions [1] of users against surveillance [2]. Currently, the Tor network is supported by thousands of volunteer relays. The popularity of Tor, a boon for online privacy, places considerable demand on network performance. Improving the network quality of service (QoS) to improve user experience is an important research topic within Tor community [3], [4], [5], [6], [7], [8], [9].

Measuring the time taken for traffic traveling from one endpoint to another, latency has a direct impact on user experience, especially for interactive applications such as web browsing and online calling [10], [11]. However, Tor often experiences higher latency than regular Internet [1], [12], [13]. A key reason is that Tor traffic is often routed through a series of geographically distributed relays. A Tor client accessing a server may construct a short, fast circuit with all intermediate relays in close proximity—or a longer, slower path spanning the globe. This routing

mechanism, while essential for Tor’s anonymity, extends the data’s journey and results in high latency [3], [9], [14], [15].

Prior work on reducing Tor latency looks at avoiding slow paths, by preferring relays that are geographically close or have historically demonstrated favorable latency performance [3], [4], [7], [8], [14], [15], [16], [17]. However, these methods may compromise Tor’s anonymity, as they undermine the randomness of circuit path, making traffic routes predictable to adversaries [18], [19], [20], [21], [22]. An alternative recent approach, ShorTor [9], incorporates extra *via relays* into conventional three-hop circuits, allowing the newly configured circuits to be faster than the standard ones. While ShorTor avoids altering Tor’s default path selection algorithm, its strategy of recruiting extra relays per circuit still introduces security risks and increases network workload. Currently, it remains an open challenge to reduce Tor’s latency without substantially compromising security or increasing network overhead.

Satellite communication, as a rapidly developing and deployed technology, provides stable and cost-effective network services to millions. The rise of satellite networks has driven research into their performance advantages and novel applications. Some studies suggest that satellite routing may offer faster transmission than terrestrial fiber, owing to its higher signal propagation speed (as explained in Appendix 1) and simpler routing structure. Consider two relays communicating with each other either via terrestrial Internet or a satellite orbiting in low-earth orbit (LEO, 550 kilometers) above the earth’s surface. In theory, satellite traffic travels at the speed of light in a vacuum via spot-beams, while terrestrial traffic may reach at most two-thirds of the speed of light in an optical fiber [23]. Disregarding node processing delays, the pure propagation latency of satellite traffic becomes lower than that of terrestrial paths when the distance between endpoints exceeds $\approx 1,100$ kilometers, as the higher signal speed offsets the longer physical path [24], [25]. In reality, satellite routing follows a simpler structure with traffic relayed by a few satellites, whereas terrestrial routing may travel across multiple network domains, resulting in a longer-than-necessary traffic journey and a higher likelihood of congestion [26], [27], [28]. Empirical measurements in the real world have also shown that satellite routing performs better than terrestrial routing in some regions [29].

The advantages of satellite routing illuminate a plausible insight to overcoming Tor’s latency challenges: by

*Haozhi Li conducted this work during a PhD visit at The University of Edinburgh.

using satellite transmissions between some relays—during the times when terrestrial network is slow—while adhering to Tor’s default path selection, it is possible to reduce latency without using extra relays in circuits or biasing circuit path. This paper presents an exploratory study on the latency of satellite-enhanced Tor (SaTor for short), aiming to answer:

Could the introduction of satellite routing technology reduce latency in the Tor network? If so, in what specific ways could Tor take this benefit?

Answering this question requires comparing satellite and terrestrial routing latencies between all pairs of Tor relays, a challenging task due to the impracticality of equipping every relay with satellite connectivity for direct latency measurements. As a solution, we developed a simulator to estimate latency via both satellite and terrestrial routing across the entire Tor network. The simulator tracks real-time satellite coordinates, identifies reachable routing paths between relay pairs, and calculates routing latency by dividing the physical path length by a probabilistic distribution of traffic speeds which is computed from public datasets of satellite and terrestrial latencies. Then, we conducted real-world measurements of SaTor latency for a subset of relay pairs using a dual-homed testbed with access to the Starlink service, capturing real satellite latency in actual Tor connections. By comparing the measured and simulated latencies, an error distribution is derived to adjust subsequent simulations. Compared to existing satellite routing simulations [30], [31], [32]—which use a constant speed of light for all latency calculations—our simulation captures both temporal and geographical characteristics in latency.

The evaluation shows that while satellite routing may not outperform terrestrial links under normal conditions, over half of relay pairs achieve notable latency reductions at tail-percentile (>90th) latencies—averaging up to 1.4 seconds, or $\approx 50\%$ lower than terrestrial latency. Since tail latencies significantly affect end-user experience [33], integrating satellite routing into Tor presents substantial potential for performance improvement. To this end, we propose a latency reduction scheme for SaTor which supposes a subset of Tor relays to be equipped with satellite network services, enabling traffic to use satellite paths when terrestrial routes are slow. This involves relays installing a satellite dish (similar to a home Wi-Fi) and subscribing to a satellite service provider, such as Starlink [34]. These dual-homed relays actively measure latency to other relays through both their satellite and terrestrial interfaces, and instruct Tor to route traffic through the faster interface by adaptively modifying the routing table in the operating system. This process, operating within the system’s network stack, requires no modifications to the existing Tor system.

The evaluation of dual-homed SaTor shows that, in a best-case scenario where all relays have satellite access, RTT latency is reduced by an average of 21.7 ms (36.6%) across all relay pairs and 41.4 ms (41.0%) across all circuits over a long-term period, with even greater gains at tail latencies. In a more realistic setup with only 100 high-bandwidth relays using satellite, SaTor still accelerates over 40% of circuits, achieving an average RTT reduction of

21.8 ms—translating to approximately 400 ms faster page load times for users. Regarding SaTor’s practicality, based on our investigation, over 94% of Tor relays are in regions with current or upcoming satellite service. While $\approx 70\%$ of relays are cloud-hosted and depend on provider support for satellite access—an area where some providers are already progressing [35], [36]—the remaining 30% of non-cloud relays are sufficient to realize a substantial portion of SaTor’s potential. With only a moderate share of relays adopting satellite access, SaTor is unlikely to increase an adversary’s network visibility compared to vanilla Tor.

Our contributions are summarized as follows:

- We propose the idea of integrating satellite routing into Tor, exploring a novel application of satellite networks and offering a fresh perspective on addressing Tor’s long-standing latency challenges.
- We present SaTor Simulator, a tool for evaluating real-time satellite and terrestrial latencies. Using globally measured datasets of satellite and terrestrial networks, we assess latency in the current Tor.
- We measured real-world terrestrial and satellite latencies in Tor to validate the advantages of satellite routing and refine the SaTor simulator.
- We propose a practical scheme for deploying satellite routing functionality in Tor and conduct a comprehensive feasibility assessment from both cost-benefit and security perspectives.

2. Background

2.1. The Tor Network

2.1.1. Onion Routing. As a key technique in Tor, onion routing encapsulates messages in multiple layers of encryption, and transmits them through a “circuit” containing a series of relays [2], [37]. Each relay decrypts a single layer to uncover the next message destination. This technique maintains the anonymity between communication endpoints, as each intermediary knows only the identity of the immediately preceding and following nodes.

A typical Tor circuit contains three relays, each selected from a large set of volunteer-operated hosts. The first relay, known as the *entry guard*, is chosen from a list of trustworthy and stable nodes, serving as the entry point for the client’s data to the Tor network. The last relay, known as the *exit relay*, is responsible for connecting Tor to the public Internet. The *middle relay* connects the entry guard to the exit to further obscure the source of the traffic.

2.1.2. Tor Latency Reduction. The end-to-end latency of a Tor circuit \mathcal{L}_{cir} primarily arises from two sources: *intra-relay processing* and *inter-relay transmission*, which can be expressed as follows:

$$\mathcal{L}_{\text{cir}} = \mathcal{L}_{\text{guard}}^{\text{P}} + \mathcal{L}_{\text{middle}}^{\text{P}} + \mathcal{L}_{\text{exit}}^{\text{P}} + \mathcal{L}_{\text{g} \rightarrow \text{m}}^{\text{T}} + \mathcal{L}_{\text{m} \rightarrow \text{e}}^{\text{T}} \quad (1)$$

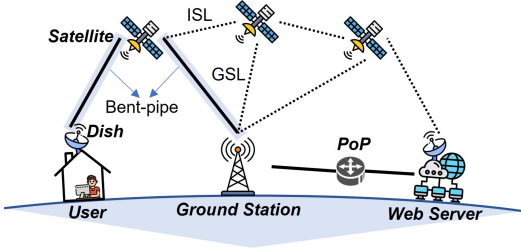


Figure 1. Overview of satellite communications.

where \mathcal{L}_X^P is the processing latency within relay X , and $\mathcal{L}_{X \rightarrow Y}^T$ means the transmission latency during the route from relay X to Y . This expression excludes latency components external to the Tor network, such as those incurred between client and guard, and between exit and the destination server.

To reduce the *intra-relay processing* latency, Tor maintains minimal hardware requirements for relays and uses a bandwidth-weighted algorithm for load balancing across relays. Further efforts may focus on optimizing the Tor software and enhancing its traffic management mechanism [6], [38], thereby reducing processing delays within relays. Moreover, the rapid growth in the number of relays can also contribute to reducing Tor’s intra-relay latency.

High *inter-relay transmission* latency is a crucial factor that hampers Tor’s performance, which is the primary focus of this paper. Such latency is closely tied to the routes of circuits. By default, Tor selects circuit routes based solely on relay bandwidth and certain security constraints [39]. This often results in slow circuits over distant geographical or heavily congested areas. A common solution involves modifying Tor’s path selection algorithm to reduce the likelihood of choosing distant or congested relays in a single circuit [3], [4], [6], [16]. However, this strategy introduces a degree of predictability into which circuits the users are likely to use, which can be exploited to narrow down the anonymity set of users, facilitating more targeted attacks for de-anonymization [40], [41], [42]. To address this challenge, this paper explores satellite routing as a potential game-changer for reducing latency in the Tor network.

2.2. Satellite Communication

Utilizing orbiting satellites to relay signals, satellite communication technology provides a way for achieving low-latency transmission. This technology has advanced notably in recent years, with an emphasis on deploying vast constellations of small, low Earth orbit (LEO) satellites to provide global, high-speed internet connectivity.

2.2.1. Routing Traffic via Satellite. The principle of satellite data routing is illustrated in Fig. 1. As shown by the solid black line, user data is transmitted from a home dish to a nearby satellite and relayed down to a ground station, forming a “bent-pipe” link structure. The data is then routed via a Point of Presence (PoP) to destination server. For the reverse path, the server’s data is sent via the PoP to the

ground station, and then to the user via satellite connection. This *single bent-pipe routing* strategy is the most fundamental approach in most satellite constellations.

Satellite routing strategies are rapidly evolving. According to Starlink’s filings, inter-satellite links (ISLs), which are laser-based connections between satellites, are being incorporated into their satellites [43], [44]. With ISLs, traffic can be relayed through multiple satellites before being transmitted to a ground station near the destination. This ISL-enabled routing retains most of the transmission path in space, where signals can, in theory, propagate at the speed of light. As a result, it offers lower latency compared to the single bent-pipe method, in which a large portion of the transmission still relies on terrestrial links.

2.2.2. Commercial LEO Satellite Constellation. Situated at an altitude ranging from 500 to 2,000 kilometers, LEO satellites enable much lower communication latency compared to traditional geostationary satellites [45]. However, the coverage of a single LEO satellite is limited, so large satellite groups must be arranged in a constellation for reliable and performant global coverage.

SpaceX’s Starlink is currently the largest low Earth orbit (LEO) satellite constellation. As of May 2025, SpaceX has launched over 8,000 satellites into orbits approximately 550 kilometers above Earth, providing service to millions of users [46], [47]. SpaceX plans to expand the Starlink constellation to as many as 34,000 satellites in the future. Eutelsat’s OneWeb is another major LEO constellation, with 660 satellites launched to an altitude of approximately 1,200 kilometers [48]. Other initiatives, including Kuiper, Yinhe, and Telesat, also have ambitious deployment plans underway. The rapid advancement of commercial LEO constellations signals a promising future for satellite-based Internet, offering potential solutions to the persistent challenges faced by conventional network applications.

2.2.3. Latency Reduction using Satellite Routing. The end-to-end latency $\mathcal{L}_{X \rightarrow Y}^T$ from relay X to relay Y , assuming the path traverses n intermediate devices $\{d_1, d_2, \dots, d_n\}$, can be modeled as:

$$\mathcal{L}_{X \rightarrow Y}^T = \mathcal{L}_{X \rightarrow d_1}^T + \sum_{i=1}^n \mathcal{L}_{d_i}^P + \sum_{i=1}^{n-1} \mathcal{L}_{d_i \rightarrow d_{i+1}}^T + \mathcal{L}_{d_n \rightarrow Y}^T \quad (2)$$

where $\mathcal{L}_{d_i}^P$ denotes the processing latency at device d_i , such as queuing delay in a router, and $\mathcal{L}_{d_i \rightarrow d_{i+1}}^T$ represents the transmission delay between devices d_i and d_{i+1} .

Compared to traditional terrestrial routing, satellite routing offers the potential to reduce both transmission latency \mathcal{L}^T and processing latency \mathcal{L}^P . Transmission latency can be estimated as the ratio of total link length to signal propagation speed. As illustrated in Fig. 1, satellite routing relays traffic through only a few satellites before reaching a ground station near the destination. In contrast, terrestrial routing often involves complex paths across multiple network domains and devices, leading to longer travel distances

and increased processing delays. Additionally, due to the physical properties of the transmission medium—satellite beam in vacuum versus optical signal in fiber—satellite traffic can theoretically propagate at the speed of light, while terrestrial traffic is limited to about two-thirds of that speed. Therefore, prior studies suggested that satellite routing would outperform terrestrial routing, particularly in long-distance transmissions [24], [25], [49], [50], [51].

In addition to the above theoretical analyses, researchers have conducted both simulative and empirical evaluations of satellite routing latency [29], [30], [31], [32], [52], [53], [54]. These studies demonstrate that satellite routing generally offers latency performance comparable to that of terrestrial routing at the current stage, and even lower latency for transmissions between certain regions. They also indicate that factors such as unstable weather conditions, satellite link reconfiguration, sub-optimal routing path, and the sparse distribution of ground stations can hinder satellite routing from realizing its full potential. However, to the best of our knowledge, no existing work has investigated the potential latency benefits and practical integration strategies of satellite routing in the context of Tor. This gap serves as the primary motivation for our work.

3. SaTor Latency Evaluation Methodology

3.1. Evaluation Goals

This paper aims to explore the potential latency reduction achieved by integrating satellite routing technology into the existing Tor. This evaluation requires estimating both satellite and terrestrial transmission latencies across all Tor relays over an extended period. The evaluation should be scalable across the entire Tor network and flexible enough to accommodate rapidly expanding satellite constellations, including both current developmental stages and future deployments. We conducted both programmatic simulation and real-world measurements, as introduced below.

3.2. Evaluation Material

The data and knowledge in evaluation includes:

Tor circuits. A Tor circuit contains two hops across three relays: entry, middle and exit. We collected a dataset containing 100,000 Tor circuits using an instrumented Tor client. The client constructs circuits using a single consensus file at 00:00 AM on December 24, 2024. These circuits include $\approx 120,000$ unique hops (relay pairs) across 6,964 relays. Our goal is to evaluate the latencies of all circuits in this dataset to assess the latency performance of the entire Tor. Since SaTor focuses exclusively on the latency between relay pairs, the circuits do not include the connections between client and entries, nor between exits and servers.

Satellite constellation. A constellation consists of satellites, ground stations, and PoPs (Fig. 1). Satellite movements are described by two-line-element (TLE) files—a standard format for recording the trajectory of earth-orbiting objects.

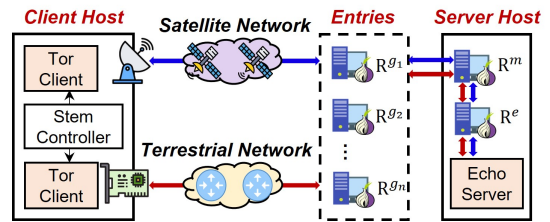


Figure 2. SaTor evaluation over real-world Tor connections.

The North American Aerospace Defense Command (NO-RAD) regularly releases the TLE files of LEO constellations, allowing for tracking real-time satellite coordinates (latitude, longitude) [55]. The coordinates of ground stations and PoPs are available on websites managed by astronomy enthusiasts [56], [57]. While these sites are unofficial, their accuracy is satisfactory for scientific research [30], [31], [32]. The evaluation is performed on Starlink constellation in December 2024, which consists of over 6,700 operational satellites, 25 PoPs, and 277 ground stations.

Baseline latency. We collect satellite and terrestrial latency measurements from public datasets as an evaluation baseline. The satellite latencies are from LENS dataset [58], which measures the ICMP RTTs between global-distributed Starlink dishes and PoPs. The LENS data we collected spans a two-month period from April to May, 2024, a total 1.624 billion data points across five geographical locations. The terrestrial latencies are sourced from RIPE Atlas, a global network to measure Internet performance [59]. We extract over 104.64 million ICMP RTT latencies from RIPE dataset, covering a one-week period starting on Sep. 2, 2024. Full data information is in Table 3 and 4, Appendix 2.

GeoIP. The geographical coordinates of each Tor relay are determined based on their IPs using GeoIP service, thus estimating the length of traffic route. The GeoIP service sources information from MaxMind dataset [60], which claims 79% and 72% of IPs are within a 100km error-range in Germany and the US, respectively, where the majority of Tor relays are located in. The coordinates of RIPE probes are provided in RIPE’s official website, deemed accurate.

3.3. Evaluation Approach

The evaluation begins with measuring satellite and terrestrial latency across a subset of Tor circuits using a real-world testbed. Next, we simulated the latencies for the same subset over a custom-built simulator, using the error between simulation and measurement to improve its accuracy. Finally, the calibrated simulator was employed to estimate the latency of Tor circuits that could not be directly measured.

3.3.1. Real-world Measurement in Tor. As shown in Fig. 2, two Tor clients, controlled by Stem library [61], run in separate Docker containers within a dual-homed host, binding to the satellite interface and the terrestrial interface, respectively. Two Tor relays, denoted as R^m and R^e , along with an echo server program, run on another host. The client

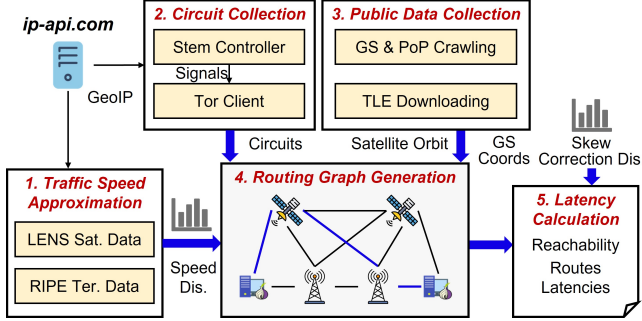


Figure 3. Procedures of simulative evaluation on SaTor.

host is in Waterloo, Canada, and the server host is in Los Angeles, USA. The two Tor clients, using the interfaces they are bound to, continuously transmit probe packets to the echo server through different circuits $c_i = \{R^{g_i}, R^m, R^e\}$, where the entry relay R^{g_i} is selected from the Tor consensus. The echo server responds immediately upon receiving each probe packet, enabling RTT calculations at the clients. This RTT primarily consists of the latency from the client to R^{g_i} (via either the satellite or terrestrial network) and from R^{g_i} to R^m (via the terrestrial network), assuming negligible latency from R^m to R^e due to their deployment on the same host. The two clients send packets through different entry relays over roughly a one-month period. By analyzing the RTTs obtained from the clients, we can derive a general comparison between satellite and terrestrial latency in Tor.

3.3.2. Programmatic Simulation. We developed a simulator to estimate the satellite and terrestrial latency between each Tor relay pairs at any given time. The core concept for calculating latency is to divide the physical length of the traffic route—determined using the geographical coordinates of endpoints—by the estimated propagation speeds of traffic. This concept is used in popular satellite routing simulators, such as Hypatia [32] and StarPerf [30]. As shown in Fig. 3, the simulator operates in five procedures:

Traffic Speed Approximation. The simulator approximates the probability distribution of satellite and terrestrial traffic speeds using the collected baseline latencies. Traffic speed is calculated as the ratio of round-trip route length to RTT latency, with sufficient RTT samples approximating the real distribution. For terrestrial traffic, the round-trip length is estimated by doubling the geographical distance between RIPE Atlas probes, whose coordinates are obtained from the Atlas official website and are considered accurate. Note that this estimation accounts only for the straight-line distance between probe pairs and does not consider the actual routing detours through intermediate devices such as routers and switches. Since traffic speeds may vary with route length, probe pairs are grouped into sub-groups based on distance, divided into 1,000-kilometer intervals, and a traffic speed distribution is separately calculated for each group.

For satellite traffic, round-trip length is estimated based on satellite routing topology. LENS latency data is measured by pinging Starlink’s PoPs from multiple client dishes,

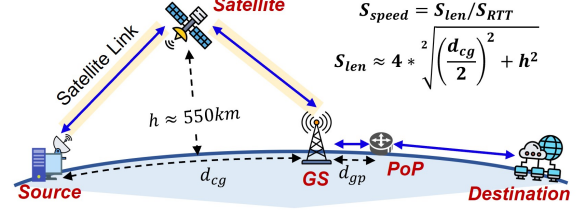


Figure 4. Satellite routing topology to estimate traffic speed.

where the PoPs serve as the gateways to local satellite networks. The traffic journey follows $client \leftrightarrow satellite \leftrightarrow groundstation \leftrightarrow PoP$, with the path $client \leftrightarrow groundstation$ over satellite links and $groundstation \leftrightarrow PoP$ on the ground. As shown in Fig. 4, the length of satellite traffic journey $S_{len} \approx 4 * \sqrt{(d_{cg}/2)^2 + h^2}$, where $h \approx 550\text{km}$ as the typical orbit altitude of LEO satellites and d_{cg} is determined through the coordinates of the client and ground station. Given that Starlink’s ground stations and PoPs are often geographically close ($d_{gp} \ll d_{cg}$), with an RTT $\approx 5\text{ms}$ [29], the satellite traffic speed is given by $S_{speed} = \frac{S_{len}}{rtt_i}$, where rtt_i is an RTT sample from the LENS dataset. Note that this RTT sample includes the 5ms groundstation-to-PoP latency, which results in a slightly underestimated satellite traffic speed, yielding a conservative estimate of satellite latency reduction benefits.

Tor Circuit Collection. Circuits are collected using an instrumented Tor client. Stem library [61] is used to send signals to the client, continuously instructing it to construct new circuits. The client is instrumented so that once a circuit is selected and saved, the relevant function will immediately return without actually building the connection. In this way, the simulator can quickly gather a large number of circuits based on up-to-date consensus file, ensuring no impact on the Tor network’s burden. Moreover, it fully leverages the most recent algorithms in the Tor system, offering an advantage over classical but outdated circuit generation tools like TorPS [62] and COGS [63]. Although the circuits are collected from a single client, given that Tor’s path selection relies on the same consensus and algorithm globally, our dataset is representative of worldwide conditions for Tor.

Public Data Collection. The TLE files for satellite constellations, along with the coordinates of ground stations and PoPs, are sourced from public websites. The TLE files are acquired from NORAD website [55], while the coordinates of ground stations and PoPs are taken from the KML file downloaded from Google Maps [56].

Routing Graph Generation. The simulator maintains a routing graph for the entire Tor network. Each node in the graph represents a communication entity, including a relay, satellite, ground station, or PoP. Note that intermediate devices along terrestrial links, such as routers and switches, are not included. Each graph edge represents a data link, with its weight corresponding to the latency between the two connected entities. This latency is estimated using the physical distance between peers and a traffic speed sampled

from the distribution obtained in Procedure 1, depending on whether the link is terrestrial (groundstation-to-PoP, PoP-to-relay) or over satellite (relay-to-satellite, satellite-to-groundstation). For terrestrial links, traffic speed is sampled from the distribution within the link’s distance interval.

At regular intervals, the simulator updates the routing graph, recalculating the coordinates of each satellite and the physical distance among nodes. It then adjusts the edge weights by resampling a speed for each link to recalculate its latency. The simulator is flexible to simulate various routing strategies of satellite constellation by switching the availability of each type of links, detailed in Appendix 3.

Latency Calculation. Using the routing graph, the latency between two relays is estimated by summing the weight of each reachable path connecting them. The simulator is designed to output the top- K shortest paths utilizing an efficient algorithm [64]. Given that Starlink may not always route traffic through the shortest path, the simulator estimates satellite routing latencies by averaging these K paths, with $K = 10$ in actual evaluations. This choice of K is sufficient for credible results, as Starlink is continuously optimizing its routing, confirmed in [65].

3.3.3. Simulation Error Correction. The simulation is based on latencies measured from global locations over an extended period, which encompass both the *transmission latency* over terrestrial fiber or satellite links, and the *processing latency* within intermediate devices such as satellites, ground stations, and routers. Continuously sampling from these latencies, our simulation replicates both spatial and temporal variability in satellite and terrestrial transmission. Compared to prior satellite routing simulators [30], [31], [32], which simply assume the speed of light for satellite links and two-thirds of the speed of light for terrestrial links, the SaTor simulator offers higher fidelity.

A potential source of simulation error arises from the fact that different protocols may exhibit differing latency characteristics. In specific, both LENS and RIPE latency measurements rely on ICMP, which may not completely reflect Tor’s TCP-based latency with multi-layer encapsulation. Unfortunately, to the best of our knowledge, no large-scale TCP-based latency measurement dataset for satellite networks is publicly available. As a solution, we use the latencies measured in our real-world testbed to calibrate the simulation results. We calculate the relative differences between the simulated and measured latencies over the same circuit path using the same interface, deriving an error distribution. For subsequent simulation, the baseline simulated latency is repeatedly adjusted by R error rates sampled from this distribution. The mean of these adjusted latencies provides the final latency estimate, while the range of these latencies is used to calculate the confidence interval.

4. SaTor Latency Reduction Scheme

A further question is: If satellite routing can outperform terrestrial routing in latency between certain relays at specific times (it can, as we will show in Section 5), how can

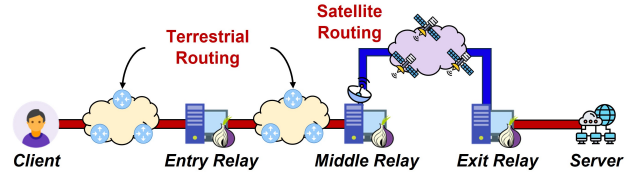


Figure 5. An illustration of circuit in SaTor.

Tor take this benefit? A naive idea is to entirely switch certain links from terrestrial to satellite routing. However, while this may reduce latency at certain times, it could increase it at others, yielding sub-optimal gains. This section presents a latency reduction scheme for SaTor, featuring adaptive dual-homing routing based on active latency measurements.

4.1. Overview

SaTor proposes equipping a subset of Tor relays with satellite network services in addition to their existing terrestrial network connections. These dual-homed relays can then communicate with other relays via satellite interfaces during periods when terrestrial routing is slow. For example, as shown in Fig. 5, a Tor client accesses a server through three relays that are selected using Tor’s default algorithm. The middle relay chooses to route traffic through satellite network to reach the exit relay, as it is considered faster than terrestrial link during that period. Thereby, with the circuit path remaining unchanged, SaTor is expected to achieve lower latency compared to the current Tor. This design requires additional hardware and software functionalities to be integrated into the current Tor, as detailed below.

4.2. SaTor Hardware Configuration

SaTor assumes that certain Tor relays install a satellite dish and subscribe to a satellite network provider, similar to purchasing a Wi-Fi router and subscribing to traditional Internet service. The new satellite interface creates a dual-homing configuration alongside the existing terrestrial interface. Relays can then route traffic to other relays through the faster interface based on real-time latency performance.

Starlink, the most widely used satellite network, offers a business plan that includes a public IP address and a personal plan that provides only a private IP [34]. A Tor relay requires a public IP to be uploaded to Tor consensus for handling inbound connections from other relays, but a private IP is sufficient for outbound connections. Therefore, SaTor can choose either plan from Starlink, provided that at least one public IP is available on either the terrestrial or satellite interface. Fig. 6 illustrates a configuration where relay *SaTorRelay1* operates a terrestrial interface (*eth0*, with public IP 129.97.7.84) and a satellite interface (*eth1*, with private IP 192.168.1.139). *SaTorRelay1* publishes its public address by setting the ‘ORPort’ and ‘Address’ fields in Tor’s configuration file, allowing inbound connections from other

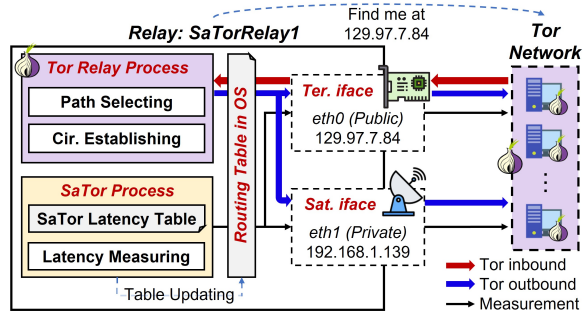


Figure 6. Routing architecture between a dual-homing SaTor relay with the remaining of Tor network.

SaTor Latency Table				Routing Table in OS	
Relay IP	Last Time	Latency Record	Measure Priority	Use Ter.	IP _i dev eth0 src 129.97.7.84 IP _j dev eth0 src 129.97.7.84
IP _i	T _i	t _{sat} ⁱ > t _{ter} ⁱ	0.8	Use Sat.	IP _k dev eth1 src 192.168.1.139 IP _l dev eth1 src 192.168.1.139
IP _k	T _k	t _{sat} ^k < t _{ter} ^k	0.1	Use Ter.	IP _i dev eth0 src 129.97.7.84 IP _j dev eth0 src 129.97.7.84
-	-	-	-	-	...

Figure 7. SaTor maintains a latency Table to record the measured latencies, and updates the system routing table to control relay’s routing behavior for reducing latency.

relays to reach *eth0*. When establishing outbound connections to other relays, *SaTorRelay1* can select between *eth0* and *eth1* for optimal latency performance. This functionality is achieved by modifying the routing table in the operating system, without requiring changes to Tor software.

If *SaTorRelay1* subscribes to Starlink’s business plan, obtaining a public IP for both satellite and terrestrial interfaces, it could upload both IPs to Tor consensus for inbound connections, similar to running two relays on a single physical host. This would allow relays without satellite access to benefit from satellite acceleration by connecting to the satellite IP of *SaTorRelay1*. However, it would require modifying Tor’s default relay selection, as some relays with satellite IPs may have to be prioritized to achieve such acceleration. Therefore, SaTor adopts the “one inbound, two outbound” configuration, as shown in Fig. 6. All changes occur after Tor’s current path selection, and relays choose fast interface solely for establishing outbound connections to the next relay. Moreover, to prevent end-to-end traffic correlation by satellite network provider, SaTor operates exclusively within the Tor network, meaning that Tor clients and exit relays do not conduct SaTor’s functionality.

4.3. SaTor Software Functionality

SaTor works as an independent program separate from the Tor system. As shown in Fig. 6, in *SaTorRelay1*, SaTor process periodically measures latency to a set of other relays through both satellite and terrestrial interfaces, maintaining a table of the measured latencies. Latency can be measured using *hping3* tool [66], by attempting to establish TCP connections to an open port of relays, as recorded in Tor’s consensus. Based on the measured latencies, the SaTor process

Algorithm 1 SaTor Latency Measuring

```

1: Define data structures:
2:   relay_list: List of all Tor relays
3:   latency_history[relay]: Historical records of the
   satellite and terrestrial latencies for each relay
4:   last_time[relay]: Last measurement time for relays
5:   priority[relay]: Measurement priority for relays
6: Function GetFasterIfaceEN(relay):
7:   psat, pter ← Probability of satellite/terrestrial inter-
   face being faster in latency_history[relay]
8:   return  $-(p_{sat} \log_2 p_{sat} + p_{ter} \log_2 p_{ter})$  // Entropy
9: Function UpdatePriority(time_now, a):
10:  for each relay ∈ relay_list:
11:    Hr ← GetFasterIfaceEN(relay)
12:    Fr ← time_now - last_time[relay]
13:    priority[relay] ← a · Hr + (1 - a) · Fr
14:  end for
15: Function MeasureLatency(relay):
16:   tsat ← Measured satellite latency to relay
17:   tter ← Measured terrestrial latency to relay
18:   latency_history[relay].append(tsat, tter)
19: Function MainLoop(T, N, a):
   // T: interval time to pause before next measurement
   // N: Maximum of relays to be measured each time
   // a: Tunable, for calculating relay measurement priority
20:  while True:
21:    time_now ← Get current time
22:    UpdatePriority(time_now, a)
23:    top_relays ← Select top n relays by priority
24:    for each relay ∈ top_relays:
25:      MeasureLatency(relay)
26:      last_time[relay] ← time_now
27:    end for
28:  sleep(t)

```

updates the routing table in operating system, connecting to some relays via the satellite interface, and others via the terrestrial. As a result, the Tor relay software, operating at the application layer, will establish new connections using the network interface specified by the system’s routing table, without requiring any code changes.

SaTor’s latency measurement, as outlined in Algorithm 1, is conducted at regular intervals *T* and measures up to *N* relays each time. Relays are prioritized for measurement based on a score calculated by the time since the last measurement and the uncertainty of the faster interface to them. This uncertainty is quantified as the entropy of the random variable for each interface being faster, based on historical records. Simply put, if the terrestrial interface is highly likely to be faster than satellite for reaching a relay, it is continuously used for communication to that relay without the need for frequent measurements. After each interval *T*, SaTor updates the priority scores, selects the top *N* relays with the highest priority, and sends probe packets through both interfaces to measure latency. Subsequently,

SaTor updates its latency table and the system’s routing table, as shown in Fig. 7. Until the next measurement cycle, Tor follows the routing table for connecting to other relays. Adjusting T and N could balance SaTor’s efficiency and effectiveness, as well as the extra workload imposed on Tor.

5. SaTor Evaluation Result

5.1. Setup Overview

The simulation was conducted on 100k Tor circuits (over 120k relay pairs), as described in Section 3.2. Each relay pair was simulated every 5 minutes over a 24-hour period, covering multiple LEO satellite orbits (≈ 100 minutes each) [24] to capture the periodic latency variations of satellite routing. The simulation adopted *ISL-enabled* routing strategy (Fig. 16(d)), as currently used in Starlink.

The SaTor latency measurement, as introduced in Section 3.3, encompasses 7,280 circuits with distinct entry relays, conducted over ≈ 30 rounds during August 2024. In each round, every circuit is measured 10 times at 1-second intervals. Finally, 7,202 and 6,915 circuits yield over 300 valid data points each and are selected to comprise the measurement dataset, which reflects the latency performance of each circuit over the one-month period.

The evaluation employs various percentiles of the latency data. For each relay pair, we obtain a simulated set containing 289 latency values and a measured set with approximately 300 data points. The 50th percentile of these latencies reflects link performance under typical conditions, values above the 95th percentile indicate performance under congested scenarios, and the 90th percentile represents the latency experienced by the majority of users [67], [68].

The evaluation is organized as follows. First, baseline traffic speeds are analyzed to offer a preliminary view of satellite and terrestrial latencies. Second, simulation and measurement are compared to derive an error distribution to correct subsequent simulations. Third, corrected simulations are performed across all circuits. Fourth, a dual-homing scenario, as proposed in Section 4, is simulated to evaluate SaTor’s best-case potential. Finally, several practical challenges in SaTor deployment are investigated.

5.2. Baseline Traffic Speed

The cumulative distribution function (CDF) for the speed of satellite and terrestrial traffic is derived from LENS and RIPE datasets, as illustrated in Fig. 15 in Appendix 2. Satellite traffic speed is calculated along actual routing paths—from the local testbed, through orbiting satellites, to a ground station. Terrestrial speeds are estimated using straight-line distances between ground-based measurement probes, due to the difficulty of predicting real-world Internet routing paths, as introduced in Section 3.2.

Overall, when the straight-line distance between endpoints is 0-2k kilometers (or 0-4k km round-trip), satellite traffic transmits faster than terrestrial traffic in most cases.

Beyond this range, terrestrial routing generally outperforms satellite routing in traffic speed, though satellite speeds still have a reasonable chance of being faster. This aligns with prior findings that long-haul terrestrial links often follow optimized backbone routes, while short paths may suffer from local congestion or inefficient inter-domain routing, leading to higher-than-necessary delays [26], [27], [28].

However, higher transmission speed of satellite traffic does not necessarily equate to lower latency, as the simulation calculates satellite latency using actual routing paths while terrestrial latency is estimated using straight-line distances. Satellite routing may only achieve lower latency when its speed advantage compensates for the longer path. An intuitive expectation is that for very short distances, terrestrial routes are too direct to be outpaced; for very long distances, terrestrial backbones are already well-optimized. But for mid-range routes—where terrestrial paths often face congestion or suboptimal routing—satellite links may bypass these issues and offer latency benefits.

5.3. Simulation Error Evaluation

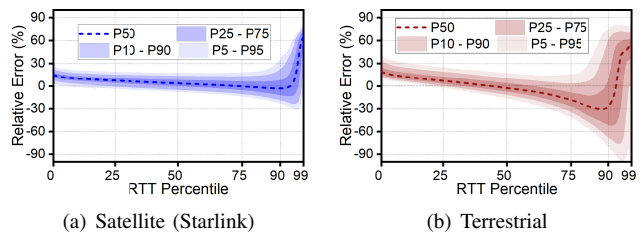


Figure 8. Relative error between simulated and measured latencies across Waterloo circuits at varying percentiles.

The traffic speed CDF enables latency estimation between two relays using their geographical distance. However, the ICMP speeds may deviate from Tor’s TCP-based, onion-routed traffic. For a given circuit, let n simulated latencies be $\mathcal{L}_s = \{l_s^1, l_s^2, \dots, l_s^n\}$ and m measured latencies be $\mathcal{L}_m = \{l_m^1, l_m^2, \dots, l_m^m\}$. The relative error at the i -th percentile is calculated as $e_i = (P_i(\mathcal{L}_m) - P_i(\mathcal{L}_s)) / P_i(\mathcal{L}_m)$. Tail percentiles typically indicate link congestion, which often leads to higher errors due to increased latency variability. We examine 5,280 circuits with both simulated and measured data. Some circuits are excluded because their relays either exited the network or changed fingerprints during the time gap between the simulation and measurement.

Fig. 8 shows the relative errors between simulated and measured latencies. The x-axis is the evaluated latency percentiles, and the y-axis displays the relative error in percentage. The dashed line shows the median error across all circuits, while the shaded regions indicate error ranges—for instance, the lightest shaded band represents the range between the 5th and 95th percentile of errors across circuits. As shown in Fig. 8(a), satellite simulations generally exhibit high fidelity. Below the 70th percentile, 90% of circuits show relative errors between $\approx -10\%$ and 25% . Beyond the 75th, the error range widens, reaching from -30% to 60% at

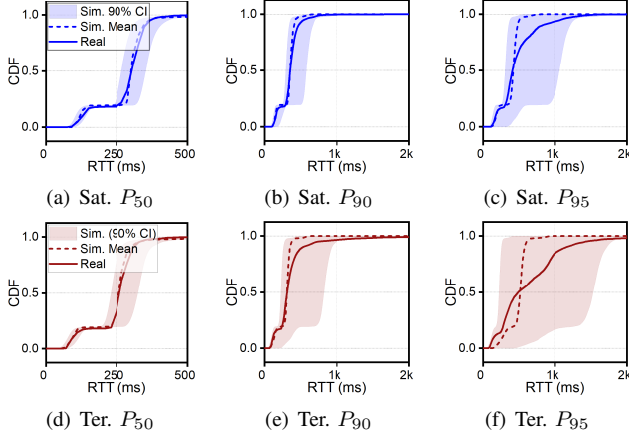


Figure 9. Latency CDFs from corrected simulations and real measurements for Waterloo-originating circuits.

the 95th. A further trend is observed beyond the 95th, where many circuits show positive errors, indicating that simulations underestimate latency compared to real measurements.

As illustrated in Fig. 8(b), below the 50th latency percentile, terrestrial simulations yield a narrow error range of roughly -15% to 40% for 90% of circuits. At the 75th, this 90% error range shifts to between -40% and 15%, while beyond the 90th, it further broadens to -90% to 70%. Across all percentiles, over 50% of circuits stay within an error range between roughly -45% to 60%, supporting the overall effectiveness of simulation. Another notable trend is that the simulation tends to overestimate real-world measurements between the 50th and 95th latency percentiles, but underestimates them beyond the 95th percentile.

Terrestrial routing simulation exhibits higher error levels than satellite routing, mainly due to its coarse-grained approach, which estimates latency using straight-line distances and overlooks the circuitous paths in the real world. In contrast, the satellite simulation tracks the precise coordinates of intermediate nodes to replicate fine-grained routing paths. Moreover, simulation discrepancies may arise from different latency properties of ICMP and Tor traffic, as well as the gap between the globally collected latency dataset and the specific latency characteristics at the measurement testbed. To mitigate this, the simulator is calibrated using the observed errors before being applied to the full Tor network.

5.4. Simulation Error Correction

At each latency percentile i , the relative errors between simulation and measurement across all circuits form a distribution \mathcal{E}_i . Then, the simulator estimates the i th percentile latency by sampling \mathcal{E}_i for R times ($R = 10k$ in the following evaluation) to adjust the baseline simulation, yielding R latency candidates. The mean of these candidates is taken as the representative estimate, while the 5th and 95th percentiles of them define a 90% confidence interval (CI).

Fig. 9 shows the CDFs of the corrected simulation and measurement for the 50th, 90th, and 95th latency percentiles.

The solid line represents the measured data, the dashed line indicates the representative latency estimate, and the shaded area denotes the 90% CI of the simulation. At the 50th percentile (Fig. 9(a) and 9(d)), the representative simulation curve closely matches the measurement. At the 90th percentile, the satellite simulation still demonstrates high fidelity (Fig. 9(b)), whereas the terrestrial simulation exhibits slight underestimation—some simulated latencies fall below the measured values (Fig. 9(e)). This trend becomes more pronounced at the 95th percentile (Fig. 9(c) and 9(f)). Nevertheless, in all cases, the 90% CI encompasses the actual measurement curve.

While repeated sampling and averaging capture overall error trends across circuits, they may smooth out deviations at the individual circuit. This becomes more pronounced in estimating tail latencies, with greater variability leading to a wider error range. Nonetheless, the simulation remains effective for capturing the overall latency distribution, even though predicting the exact error for each individual circuit is inherently difficult. The measurement at a single location should be interpreted as a specific instance within the CI, rather than a contradiction of the simulation model, which is designed to capture global-scale characteristic.

Based on the corrected simulations and measurements, the relative reduction between satellite latency (l_{sat}) and terrestrial latency (l_{ter}), computed as $(l_{\text{ter}} - l_{\text{sat}}) / l_{\text{ter}} \times 100\%$, is shown in Table 1. Blue text indicates underestimation by the simulation (more circuits actually experience such level of reduction), while red indicates overestimation. At the 50th percentile, the measurement shows that 0.11% of circuits achieve a significant reduction ($>20\%$), whereas the simulation reports none. At the 95th, the simulation overestimates this figure at 80.65%, compared to the measured 60.70%. However, this overestimation only occurs in the 20–40% reduction range, as the simulation actually underestimates the number of circuits achieving larger reductions. Overall, the calibrated simulator is expected to *conservatively* estimate satellite’s latency reduction when applied to large-scale simulations across the entire Tor.

5.5. Satellite and Terrestrial Latency in Tor

Fig. 10(a)–10(f) present the latency histograms for all 120k relay pairs, focusing on tail latencies at the 90th, 95th, and 98th percentiles. Lower percentiles are omitted, at which satellite routing showed limited latency reduction in the measurements. At the 90th percentile, satellite and terrestrial routing exhibit similar latency distributions. At the 95th, satellite routing demonstrates latency reduction efficacy, with a slightly smaller proportion of relay pairs exceeding 250 ms compared to terrestrial routing. At the 98th percentile, its effectiveness becomes more pronounced, eliminating all tail pairs with latencies over 1k ms and reducing the number of pairs exceeding 250 ms.

Table 2 presents the percentage relative latency reduction of satellite routing compared to terrestrial routing. At the 90th percentile, approximately 0.53% of relay pairs show significant reductions ($>20\%$), with an average reduction

TABLE 1. SIMULATED AND MEASURED LATENCY REDUCTION AFTER USING SATELLITE ROUTING FOR WATERLOO-ORIGINATING CIRCUITS

Percentile	Relative Reduction (%)					Sum. >20	Ave. Reduction
	<20	20-40	40-60	60-80	80-100		
50th	100.00% (99.89) ¹	0.00% (0.03)	0.00% (0.04)	0.00% (0.04)	0.00% (0.00)	0.00% (0.11)	0.00% (48.95)
90th	97.06% (79.72)	2.35% (5.88)	0.00% (4.12)	0.00% (5.90)	0.59% (4.38)	2.37% (20.28)	25.06% (57.89) ²
95th	19.01% (39.30)	71.38% (10.96)	8.55% (18.84)	0.47% (24.94)	0.59% (5.96)	80.65% (60.70)	29.93% (58.08)

¹ Indicating that for the 50th percentile latency throughout simulation period, 99.41% of circuits show < 20% reduction after using satellite, while this result is 99.89% in the real measurement under the same conditions.

² Among relay pairs that exhibit significant latency reduction (> 20%), satellite routing is, on average, 25.06% faster compared to terrestrial routing. This result is 57.89% in the real measurements.

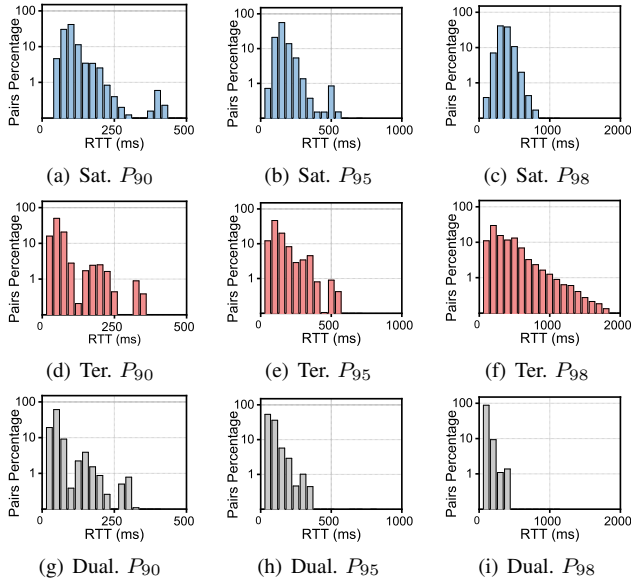


Figure 10. Simulated latency histo. for pairs using satellite (a-c), terrestrial (d-f), and dual-homing routing (g-i).

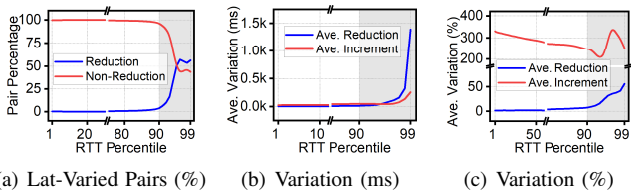


Figure 11. Simulated latency variation using satellite routing across the 1-99th percentile throughout simulation.

of 24.39%. This share increases to 18.06% at the 95th and 30.35% at the 98th. Fig. 11 illustrates the overall latency reduction of satellite routing across 1-99th percentiles. Satellite routing begins to show notable latency reduction above the 90th percentile, and at the 99th, it accelerates over 55% of relay pairs by an average of 1.4s (or 50%). However,

TABLE 2. SIMULATED LATENCY REDUCTION OF SATELLITE ROUTING

P	Relative Reduction (%)					Ave.
	<20	20-40	40-60	60-80	>20	
90th	99.47%	0.53%	0.00%	0.00%	0.00%	24.39%
95th	81.95%	13.28%	4.48%	0.29%	0.00%	34.26%
98th	69.66%	10.84%	9.62%	8.10%	1.78%	49.85%

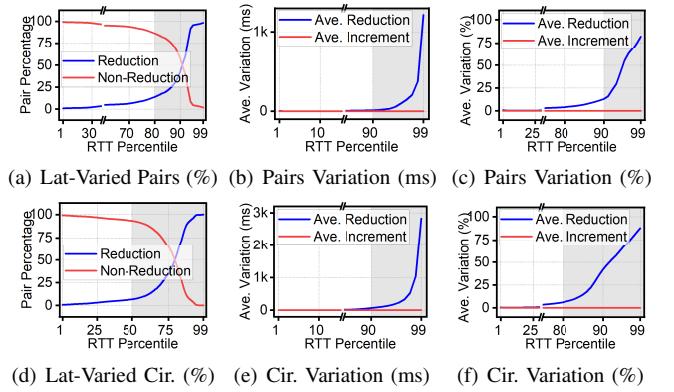


Figure 12. Simulated latency variation in dual-homed SaTor, at relay pair (a-c) and circuit (d-f) level.

it is worth noting that a comparable portion of relay pairs ($\approx 45\%$ at the 99th) experience no latency reduction—and in fact suffer from an average latency increase of nearly $3\times$ —when switching from terrestrial to satellite routing, as shown by the red line in the figures.

Satellite acceleration efficacy is found to be most pronounced for pairs with geographic distances between 0.5–1k km and 5–6k km. A possible explanation is that, in the former range, elevated terrestrial latencies are likely caused by local congestion or inefficient routing across regional ASes. In the latter, inter-satellite links in satellite network outperform transoceanic terrestrial paths, offering improved performance. A detailed discussion is in Appendix 4. A further finding is that, at tail percentiles, links benefiting from satellite acceleration exhibit high absolute latency reduction (in ms) but low relative reduction (%). Conversely, links not improved by satellite show low absolute but high relative latency increases. This suggests that satellite routing is effective for high-latency connections but may slow down links which are already fast on terrestrial path.

5.6. Dual-Homing Latency in SaTor

The preceding evaluation confirms SaTor’s latency advantages, particularly in tail latencies that critically impact user experience. The dual-homing scheme proposed in Section 4 suggests equipping relays with satellite access alongside their existing terrestrial connectivity, enabling real-time interface switching for latency optimization. The evaluation

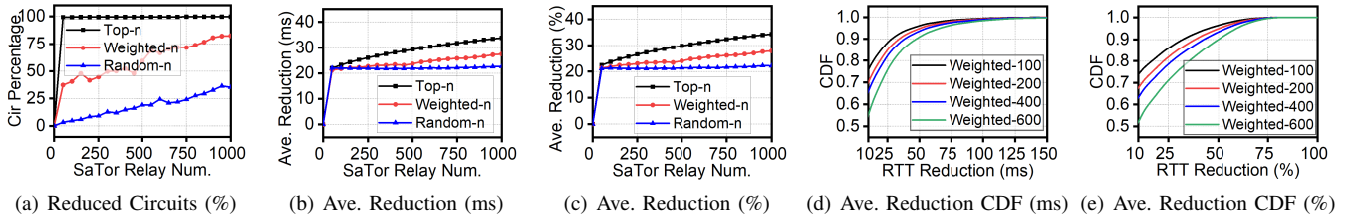


Figure 13. Circuit-level latency reduction of dual-homed SaTor in the three deployment scenarios, using $N = 50$ and $T = 5$.

begins by envisioning an ideal scenario in which all relays are dual-homed, providing a best-case estimate.

As shown in Fig. 10(g)–10(c), dual-homing routing outperforms both single-homing satellite and terrestrial routing, effectively mitigating high-tail latency across all relay pairs. Fig. 12 presents the overall latency reduction achieved by integrating the dual-homing routing scheme in SaTor, at both relay-pair and circuit levels. In this setup, the SaTor software periodically probes latency to 50 other relays at 5-minute intervals. It is found that nearly all links exhibit latency reduction, especially at tail percentiles, with latency degradation observed in only a negligible fraction. This aligns with expectations, as the relay can keep selecting the faster interface throughout the simulation. In particular, at the 99th percentile, over 98% of pairs show an expected latency reduction of over ≈ 1.2 seconds (82%), with almost all circuits showing ≈ 2.8 seconds (87.9%). Using the average across all percentiles as a metric, SaTor scheme achieves an expected latency reduction of ≈ 21.7 ms (36.6%) at a relay-pair level and ≈ 41.4 ms (41.0%) at a circuit level.

5.7. Incremental Deployment of SaTor

Equipping all relays with satellite service, as assumed in the previous evaluation, is a costly endeavor. This subsection evaluates whether deploying satellite access to a small subset of relays can still deliver meaningful benefits. The evaluation considers three deployment scenarios: *top-n*, *weighted-n*, and *random-n*. The *top-n* scenario assumes that the n relays with the highest likelihood of being selected adopt satellite connectivity, achieving highest efficacy with minimal investment. The *weighted-n* assumes that relays adopt satellite with a probability proportional to their normalized bandwidth—higher-bandwidth relays have a greater incentive and resources to invest in SaTor. In the *random-n* scenario, relays adopt satellite independently at random.

As shown in Fig. 13(a)–13(c), in the *top-n* scenario, equipping just 50 relays with SaTor functionality accelerates over 99.3% of circuits, achieving an expected latency reduction of ≈ 21.9 ms (22.4%), still measured as the average across all percentiles. Expanding to top 1k relays yields an expected reduction of ≈ 33.9 ms (34.3%) across all circuits. In the *weighted-n* scenario, ≈ 350 SaTor relays achieve an expected reduction of ≈ 23.1 ms (23.4%) for 50.1% of circuits, while 1k relays benefit 82.5% of circuits with an average of 27.5 ms (27.8%). The *random-n* shows the least efficacy: even with 1k SaTor relays, only 35.2% of circuits are accelerated with an average of 22.6 ms (22.1%).

Fig. 13(d) shows the CDF of absolute latency reduction across all circuits under the *weighted-n* scenario—the most reasonable assumption in practice. With 100 SaTor relays, $\approx 24\%$ of circuits show a latency reduction greater than 10 ms, 3.95% exceed 50 ms, and 0.07% exceed 100 ms. When using 600 SaTor relays, 44.5% of circuits show a reduction greater than 10 ms, 9.1% exceed 50 ms, and 1.2% exceed 100 ms. In terms of relative reduction (Fig. 13(e)), deploying 600 SaTor relays yields a $>10\%$ latency reduction for 47.2% of circuits, $>25\%$ for 29.9%, and $>50\%$ for 10.1%.

Regarding the real-world feasibility of SaTor deployment, over 94% of relays are located in regions where Starlink service is either available or expected to be available soon. Moreover, based on the data from Tor metrics [1] and IPinfo database [69], cloud platforms host over 70% of relays, followed by general ISPs (20%), business (3%), and education networks (7%). While deploying SaTor on cloud-hosted relays may require collaboration with satellite providers, major cloud companies are already partnering with satellite services, facilitating potential deployment [35], [36]. On non-cloud relays (30% of all relays), direct access to physical machines makes satellite installation simpler. Detailed discussion is provided in Appendix 5.

5.8. Cost of SaTor

SaTor requires the *financial investment* for equipping relays with satellite service, and the *extra bandwidth* required for real-time latency measurements. Currently, satellite networks are widely deployed by several commercial companies, providing services to millions with comparable cost to traditional terrestrial networks. For example, Starlink offers a minimum monthly subscription fee of 80 USD [47], while fiber subscriptions may range from 50 to 100 USD per month [70]. With Starlink’s rapid expansion, satellite costs are expected to decrease further. Regarding additional bandwidth cost, assuming each SaTor relay sends a probe packet via both satellite and terrestrial interfaces to 50 other relays every 5 minutes, the total bandwidth consumption is roughly 3MB per relay per day—a minimal overhead compared to Tor’s recommended relay bandwidth [71]. Running in an independent process and modifying the system’s routing table, SaTor can achieve all its functions without requiring modifications to the Tor application itself.

6. SaTor Security Analysis

6.1. Adversary Model

SaTor considers two adversaries: *relay-level*, referring to malicious relays, and *network-level*, denoting adversarial network service providers. A *relay-level* adversary may actively manipulate traffic to disrupt Tor functionality [72], or passively analyze metadata—such as packet size and timing—for deanonymization through website fingerprinting techniques [73]. An adversary controlling both the entry and exit relay of a circuit can perform end-to-end correlation attacks to deanonymize users [74]. A *network-level* adversary typically conducts passive surveillance and may attempt AS-level correlation by observing both ends of circuits from different vantage points [75], [76]. In restrictive scenarios, state-level actors may drop connections to known relays or block Tor protocol signatures, limiting user access to Tor [77]. Multiple network-level adversaries may also collude, increasing their traffic visibility and attack effectiveness.

An adversary’s advantage is measured by the proportion of connections it observes—a prerequisite for most known attacks. SaTor’s security implications are assessed using *differential advantage*, which measures the additional benefit an adversary gains after introducing satellite routing in Tor.

6.2. Malicious Relays

SaTor preserves Tor’s default path selection and only opportunistically employs satellite on certain hops within the default circuit. The presence of satellite interfaces does not confer any selection priority. Hence, malicious relays in SaTor appear in circuits with the same probability as in vanilla Tor and gain no additional visibility. While a malicious SaTor relay may attempt to undermine latency benefits by consistently avoiding, or exclusively using, satellite interfaces, such misbehavior is not unique to SaTor. Comparable actions—such as deliberate throttling—can also be carried out by relays in vanilla Tor. Therefore, SaTor is unlikely to increase the capabilities of relay-level adversaries.

6.3. Adversarial Satellite Service Provider

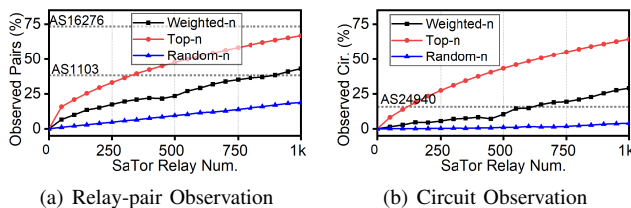


Figure 14. Observable relay pairs and circuits from satellite providers and from major terrestrial providers.

Satellite services are dominated by a few providers, which may act as new network-level adversaries introduced

by SaTor. However, in terms of threat model, these satellite providers are fundamentally similar to traditional fiber-based providers. Currently, Tor is unevenly distributed, with many relays hosted by a small number of providers [1]. In SaTor, as long as satellite deployment remains moderate, satellite providers do not gain undue advantage. Fig. 14(a) shows the percentage of relay pairs observable by satellite providers under varying numbers of SaTor relays, alongside the visibility of the two most dominant terrestrial providers. To match AS1103’s visibility (40% of pairs), the weighted-n scenario requires 900 satellite relays, while the top-n scenario requires 350. To reach AS16276’s visibility (70%), both scenarios require over 1k satellite relays.

Circuit observation is defined as the case where the entire entry-to-exit path is visible to the adversary. A terrestrial network operator achieves this simply by hosting a middle relay and observing its ingress and egress traffic. In contrast, a satellite provider must host both the entry and middle, since SaTor uses satellite only for outbound connections. Exits are excluded as Tor disallows one operator from hosting both entry and exit, and SaTor prevents satellite usage at exits. As shown in Fig. 14(b), matching AS24940’s visibility (15.68% of circuits) requires >600 satellite relays in the weighted-n scenario and ≈ 150 in the top-n.

Combined with the findings in Section 5.7, SaTor achieves reasonable benefits with less than one hundred dual-homed relays, without posing significant advantages to satellite providers. Moreover, SaTor can tolerate a greater number of satellite relays by distributing them across different providers, such as Starlink [47], OneWeb [48], and Amazon Kuiper [78], thereby avoiding excessive visibility by any single entity. Moreover, recall that SaTor only modifies the data forwarding process between entry and exit relays, leaving the connections between client and entry, as well as between exit and destination server, unchanged. Therefore, SaTor does not increase the risk of end-to-end deanonymization attacks, which require a global adversary capable of observing both ends of a circuit. To this end, *Collusion* with satellite providers, whether by other network operators or malicious relays, is fundamentally similar to collusion with fiber-based providers. Introducing satellite routing into Tor simply implies a small subset of relays migrating to a few new providers, whether satellite or terrestrial-based.

6.4. Fingerprinting Attacks in SaTor

Attackers can infer the websites users visit by analyzing traffic at entry relays, exploiting the fact that traffic metadata varies across websites. Since satellite transmissions may introduce distinguishable traffic metadata compared to terrestrial links, it is important to reassess SaTor’s vulnerability to website fingerprinting. Encouragingly, a recent study [79] finds that Tor over Starlink is comparably susceptible to website fingerprinting as Tor over fiber. By collecting traffic datasets from both terrestrial and Starlink connections to the Tor network, the study observed that state-of-the-art fingerprinting attacks show a $\approx 2\text{--}8\%$ drop in accuracy over satellite links. Furthermore, fingerprinting defenses are

similarly, or even more effective on Starlink, reducing attack accuracy by up to 12% more than on fiber.

Satellite traffic may be fingerprinted for *relay discovery*. For instance, an exit relay could infer satellite transmission between the guard and middle by detecting satellite-specific metadata. The use of satellite may help the exit to narrow down the guard’s location, as satellite acceleration often correlates with geographic factors. A mitigation is to expand satellite usage across more links by allowing relays to use satellite even if they are $< t\%$ slower, trading some performance for security. However, this does not increase satellite providers’ visibility beyond Fig. 14, which accounts for any link involving satellite-equipped relays, regardless of whether satellite routing is used in the simulation.

7. Discussion

Bandwidth versus Latency. As introduced in Section 2.1.2, this paper focuses exclusively on *inter-relay* latency, which is determined by the characteristics of the underlying network paths between relays—such as physical distance and routing topology—rather than the bandwidth of individual relays. Thus, our evaluation disregards variations in relay bandwidth, as they have little impact on SaTor’s effectiveness, given that SaTor introduces only minimal ($\approx 3\text{MB}$ per relay per day) extra bandwidth overhead.

Practical Impact on User Experience. The evaluation uses RTT latency, which may not directly reflect SaTor’s benefits from an end-user perspective. Based on [9], a 50 ms RTT reduction roughly corresponds to a 1 second ($\approx 20\times$) page-load-time (PLT) improvement during web browsing. With 100 SaTor relays in the weighted- n scenario, $\approx 40.5\%$ of circuits see an average RTT reduction of 21.8 ms (Fig. 13), translating to an expected ≈ 400 ms PLT minimization. Also, 3.95% of circuits see >50 ms RTT reduction and 0.7% exceed 100 ms, implying >1 s and >2 s PLT improvements, respectively. Notably, these figures are averaged across all percentiles. SaTor’s impact at tail latencies—those most affecting user experience—would be more significant.

A Secondary Satellite Link versus Terrestrial Link. SaTor’s adaptive switching between dual interfaces can be extended to broader scenarios, i.e., dual terrestrial links from different providers. However, the feasibility of this approach depends on the independence of latency variation across the dual links. If both paths degrade under similar network congestion, switching brings limited benefit. This is where satellite routing becomes uniquely advantageous. Local terrestrial providers often share inter-domain infrastructure, such as Internet Exchange Points (IXPs) and transit backbones, making them susceptible to correlated congestion [80], [81], [82]. In contrast, satellite paths operate on a distinct physical layer and can bypass congested terrestrial segments, routing data closer to the destination with minimal overlap. Given that inter-domain congestion is an important contributor to Internet latency [83], [84]—and that Tor frequently constructs long-distance, cross-domain circuits—the physical and topological independence of satellite routing makes it a compelling complement to terrestrial links.

8. Related Work

Tor’s latency reduction efforts can be categorized as *biased* or *non-biased*. The *biased* approaches prioritize links with lower latency, based on either ad-hoc measuring prior to link selection or historical latency records. Instead of Tor’s default relay-by-relay selection, these approaches often perform circuit-level selection [7], [8], [15], [17], evaluating the overall performance of candidate circuits and assigning higher selection weights to those with lower latency. Such active manipulation on circuit selection often yields notable latency improvements, e.g., PredicTor [8] accelerates 10% of circuits by >1.5 s in PLT, while SaTor achieves only a >600 ms reduction for 10% using 100 weighted- n relays.

However, the biased approaches impose additional predictability to users’ data paths, offering advantage to adversaries. Algorithms favoring geographically short circuits might exacerbate the node-placement attack, wherein adversaries position malicious nodes close to users to increase their chances of being selected [20], [22]. Passive attackers, who deanonymize users by monitoring the latency or speed of a circuit, now only need to observe fewer circuits to make accurate inferences [18], [19], [85], [86]. For Tor, which relies on a large and diverse user base to maintain anonymity, reduction in the randomness of user behavior could heighten deanonymization risk [40], [41], [42].

The *non-biased* approaches retain Tor’s default path selection algorithm, while modifying the subsequent data routing process. Multi-path routing approaches split traffic across multiple semi-disjoint circuits to avoid single-path congestion, based on the fact that due to the heterogeneity of relay bandwidths, some relays are heavily used while others are less traveled [5], [87]. However, simultaneously using multiple circuits increases vulnerability to end-to-end correlation attacks by broadening the exposure to network-level adversaries and malicious relays, which may deanonymize users by observing just one sub-circuit. In contrast, SaTor does not introduce additional relays or alter the end segments of circuits, thereby avoiding extra correlation risks.

Another non-biased approach, *ShorTor*, adds extra *via relays* into standard circuits, to make the newly built circuit faster [9]. Although ShorTor effectively reduces Tor latency without significant security compromises, its effectiveness is largely concentrated in a small fraction of circuits. Concretely, it reduces latency by >100 ms for 1.1% of circuits, >25 ms for 8%, and >10 ms for 11%, while the remaining 90% show no significant improvement. In comparison, SaTor under the weighted-100 scenario improves latency by over 100 ms for 0.7% of circuits, over 25 ms for 14%, and over 10 ms for 24%, with $\approx 40\%$ of circuits experiencing improvements. Additionally, ShorTor may impose a non-negligible burden on Tor by requiring some relays to manage traffic that would not ordinarily be routed through them. It also consumes ≈ 100 MB of additional bandwidth per relay per day, while SaTor requires only 3 MB.

9. Conclusion

High latency remains an essential challenge for Tor. Traditional latency reducing strategies often bias shorter circuits, compromising traffic path randomness and degrading security. This paper explores satellite routing in Tor, outfitting relays with satellite connections, coupled with a dual-homing mechanism to adaptively arrange the usage of satellite and terrestrial interfaces for optimal latency. Our evaluation shows that over a long-term observation, SaTor in general accelerates over 40% circuits by an average of 21.8 ms, with the top 100 most popular relays accessed to satellite network. This study offers a first perspective on utilizing satellite technology to address Tor's challenges, serving as a reference for Tor's future improvements.

References

- [1] T. T. Project, "Tor metrics." <https://metrics.torproject.org/>, 2025. Online.
- [2] R. Dingledine, N. Mathewson, P. F. Syverson, *et al.*, "Tor: The second-generation onion router," in *USENIX security symposium*, vol. 4, pp. 303–320, 2004.
- [3] M. Akhondi, C. Yu, and H. V. Madhyastha, "LASTor: A low-latency AS-aware Tor client," in *2012 IEEE Symposium on Security and Privacy*, pp. 476–490, IEEE, 2012.
- [4] T. Wang, K. Bauer, C. Forero, and I. Goldberg, "Congestion-aware path selection for Tor," in *Financial Cryptography and Data Security: 16th International Conference, FC 2012, Kralendijk, Bonaire, February 27-March 2, 2012, Revised Selected Papers 16*, pp. 98–113, Springer, 2012.
- [5] M. AlSabah, K. Bauer, T. Elahi, and I. Goldberg, "The path less travelled: Overcoming Tor's bottlenecks with traffic splitting," in *Privacy Enhancing Technologies: 13th International Symposium, PETS 2013, Bloomington, IN, USA, July 10-12, 2013. Proceedings 13*, pp. 143–163, Springer, 2013.
- [6] M. AlSabah and I. Goldberg, "Performance and security improvements for Tor: A survey," *ACM Computing Surveys (CSUR)*, vol. 49, no. 2, pp. 1–36, 2016.
- [7] R. Annessi and M. Schmiedecker, "NavigaTor: Finding faster paths to anonymity," in *2016 IEEE European Symposium on Security and Privacy (EuroS&P)*, pp. 214–226, IEEE, 2016.
- [8] A. Barton, M. Wright, J. Ming, and M. Imani, "Towards predicting efficient and anonymous Tor circuits," in *27th USENIX Security Symposium (USENIX Security 18)*, pp. 429–444, 2018.
- [9] K. Hogan, S. Servan-Schreiber, Z. Newman, B. Weintraub, C. Nita-Rotaru, and S. Devadas, "ShorTor: Improving Tor network latency via multi-hop overlay routing," in *2022 IEEE Symposium on Security and Privacy (SP)*, pp. 1933–1952, IEEE, 2022.
- [10] N. J. Taylor, A. R. Dennis, and J. W. Cummings, "Situation normality and the shape of search: The effects of time delays and information presentation on search behavior," *Journal of the American Society for Information Science and Technology*, vol. 64, no. 5, pp. 909–928, 2013.
- [11] I. Arapakis, X. Bai, and B. B. Cambazoglu, "Impact of response latency on user behavior in Web search," in *Proceedings of the international ACM SIGIR conference on Research & development in information retrieval*, pp. 103–112, 2014.
- [12] R. Dingledine and S. J. Murdoch, "Performance improvements on Tor or, why Tor is slow and what we're going to do about it," Online: <http://www.torproject.org/press/presskit/2009-03-11-performance.pdf>, p. 68, 2009.
- [13] P. Dhungel, M. Steiner, I. Rimac, V. Hilt, and K. W. Ross, "Waiting for anonymity: Understanding delays in the Tor overlay," in *2010 IEEE Tenth International Conference on Peer-to-Peer Computing (P2P)*, pp. 1–4, IEEE, 2010.
- [14] C. Wacek, H. Tan, K. S. Bauer, and M. Sherr, "An empirical evaluation of relay selection in Tor," in *Proceedings of the Network and Distributed System Security Symposium*, 2013.
- [15] M. Imani, M. Amirabadi, and M. Wright, "Modified relay selection and circuit selection for faster Tor," *IET Communications*, vol. 13, no. 17, pp. 2723–2734, 2019.
- [16] R. Snader and N. Borisov, "A tune-up for tor: Improving security and performance in the Tor network," in *Proceedings of the Network and Distributed System Security Symposium*, vol. 8, p. 127, 2008.
- [17] M. Sherr, M. Blaze, and B. T. Loo, "Scalable link-based relay selection for anonymous routing," in *Privacy Enhancing Technologies: 9th International Symposium, PETS 2009, Seattle, WA, USA, August 5-7, 2009. Proceedings 9*, pp. 73–93, Springer, 2009.
- [18] P. Mittal, A. Khurshid, J. Juen, M. Caesar, and N. Borisov, "Stealthy traffic analysis of low-latency anonymous communication using throughput fingerprinting," in *Proceedings of the 18th ACM conference on Computer and Communications Security*, pp. 215–226, 2011.
- [19] A. Houmansadr and N. Borisov, "SWIRL: A scalable watermark to detect correlated network flows," in *Proceedings of the Network and Distributed System Security Symposium*, Citeseer, 2011.
- [20] G. Wan, A. Johnson, R. Wails, S. Wagh, and P. Mittal, "Guard placement attacks on path selection algorithms for Tor," *Proceedings on Privacy Enhancing Technologies*, vol. 2019, no. 4, 2019.
- [21] I. Karunanayake, N. Ahmed, R. Malaney, R. Islam, and S. K. Jha, "De-anonymisation attacks on Tor: A survey," *IEEE Communications Surveys & Tutorials*, vol. 23, no. 4, pp. 2324–2350, 2021.
- [22] Q. Tan, X. Wang, W. Shi, J. Tang, and Z. Tian, "An anonymity vulnerability in Tor," *IEEE/ACM Transactions on Networking*, vol. 30, no. 6, pp. 2574–2587, 2022.
- [23] C. Incorporated, "Smf-28tm optical fiber product information," 2002.
- [24] M. Handley, "Delay is not an option: Low latency routing in space," in *Proceedings of the 17th ACM Workshop on Hot Topics in Networks*, pp. 85–91, 2018.
- [25] M. Handley, "Using ground relays for low-latency wide-area routing in megaconstellations," in *Proceedings of the 18th ACM Workshop on Hot Topics in Networks*, pp. 125–132, 2019.
- [26] I. N. Bozkurt, A. Aguirre, B. Chandrasekaran, P. B. Godfrey, G. Laughlin, B. Maggs, and A. Singla, "Why is the Internet so slow?!", in *Passive and Active Measurement: 18th International Conference, PAM 2017, Sydney, NSW, Australia, March 30-31, 2017, Proceedings 18*, pp. 173–187, Springer, 2017.
- [27] T. Høiland-Jørgensen, B. Ahlgren, P. Hurtig, and A. Brunstrom, "Measuring latency variation in the Internet," in *Proceedings of the 12th International Conference on emerging Networking Experiments and Technologies*, pp. 473–480, 2016.
- [28] J. Chavula, A. Phokeer, A. Formoso, and N. Feamster, "Insight into Africa's country-level latencies," in *IEEE AFRICON 2017*, pp. 938–944, Institute of Electrical and Electronics Engineers Inc., 2017.
- [29] N. Mohan, A. Ferguson, H. Cech, P. R. Renatin, R. Bose, M. Marina, and J. Ott, "A multifaceted look at Starlink performance," in *Proceedings of the ACM Web Conference 2024 (WWW '24)*, 2024.
- [30] Z. Lai, H. Li, and J. Li, "StarPerf: Characterizing network performance for emerging mega-constellations," in *2020 IEEE 28th International Conference on Network Protocols (ICNP)*, pp. 1–11, IEEE, 2020.
- [31] Z. Lai, H. Li, Y. Deng, Q. Wu, J. Liu, Y. Li, J. Li, L. Liu, W. Liu, and J. Wu, "StarryNet: Empowering researchers to evaluate futuristic integrated space and terrestrial networks," in *20th USENIX Symposium on Networked Systems Design and Implementation (NSDI 23)*, pp. 1309–1324, 2023.

- [32] S. Kassing, D. Bhattacharjee, A. B. Águas, J. E. Saethre, and A. Singla, "Exploring the Internet from space with Hypatia," in *Proceedings of the ACM Internet Measurement conference*, pp. 214–229, 2020.
- [33] A. Cloud, "Performance monitoring metrics." <https://www.alibabacloud.com/help/en/well-architected/latest/performance-monitoring-indicators/>, 2025. Online.
- [34] Starlink, "Starlink service plans." <https://www.starlink.com/service-plans/>, 2025. Online.
- [35] D. Mohney, "The space cloud: Satellite strategies for AWS, Google and Microsoft." <https://www.datacenterfrontier.com/cloud/article/11428161/the-space-cloud-satellite-strategies-for-aws-google-and-microsoft>, 2021.
- [36] A. Raj, "How satellites are becoming a game changer for cloud service providers." <https://techwireasia.com/03/2023/heres-how-satellites-are-enhancing-connectivity-for-cloud-service-providers/>, 2023.
- [37] M. G. Reed, P. F. Syverson, and D. M. Goldschlag, "Anonymous connections and onion routing," *IEEE Journal on Selected areas in Communications*, vol. 16, no. 4, pp. 482–494, 1998.
- [38] R. Jansen, P. Syverson, and N. Hopper, "Throttling Tor bandwidth parasites," in *21st USENIX Security Symposium (USENIX Security 12)*, pp. 349–363, 2012.
- [39] R. Dingledine and N. Mathewson, "Tor specifications," 2023.
- [40] M. Backes, A. Kate, S. Meiser, and E. Mohammadi, "(Nothing else) MATor(s): Monitoring the Anonymity of Tor's Path Selection," in *Proceedings of the 21th ACM conference on Computer and Communications Security (CCS 2014)*, November 2014.
- [41] M. Backes, S. Meiser, and M. Slowik, "Your Choice MATor(s): Large-scale quantitative anonymity assessment of Tor path selection algorithms against structural attacks," *Proceedings on Privacy Enhancing Technologies*, vol. 2016, April 2016.
- [42] J. Juen, A. Johnson, A. Das, N. Borisov, and M. Caesar, "Defending Tor from network adversaries: A case study of network path prediction," *Proceedings on Privacy Enhancing Technologies*, vol. 2015, no. 2, pp. 1–17, 2015.
- [43] SpaceX FCC update, "SPACEX NON-GEOSTATIONARY SATELLITE SYSTEM." https://licensing.fcc.gov/myibfs/download.do?attachment_key=1569860, 2018. Online.
- [44] Michael Kan, "SpaceX Launches Upgraded Starlink Satellites Featuring Laser Links." <https://uk.pcmag.com/networking/135644/spacex-launches-upgraded-starlink-satellites-featuring-laser-links>, 2021. Online.
- [45] Y. Su, Y. Liu, Y. Zhou, J. Yuan, H. Cao, and J. Shi, "Broadband leo satellite communications: Architectures and key technologies," *IEEE Wireless Communications*, vol. 26, no. 2, pp. 55–61, 2019.
- [46] J. McDowell, "Jonathan's Space Report." <https://planet4589.org/>, 2025. Online.
- [47] SpaceX, "Starlink." <https://www.starlink.com/>, 2025. Online.
- [48] OneWeb, "Oneweb." <https://oneweb.net/>, 2025. Online.
- [49] A. U. Chaudhry and H. Yanikomeroğlu, "Optical wireless satellite networks versus optical fiber terrestrial networks: The latency perspective: Invited chapter," in *30th Biennial Symposium on Communications 2021*, pp. 225–234, Springer, 2022.
- [50] A. U. Chaudhry and H. Yanikomeroğlu, "On crossover distance for optical wireless satellite networks and optical fiber terrestrial networks," in *2022 IEEE Future Networks World Forum (FNWF)*, pp. 480–485, IEEE, 2022.
- [51] G. Giuliani, T. Ciussani, A. Perrig, and A. Singla, "ICARUS: Attacking low earth orbit satellite networks," in *2021 USENIX Annual Technical Conference (USENIX ATC 21)*, pp. 317–331, 2021.
- [52] M. M. Kassem, A. Raman, D. Perino, and N. Sastry, "A browser-side view of Starlink connectivity," in *Proceedings of the 22nd ACM Internet Measurement Conference*, pp. 151–158, 2022.
- [53] S. Ma, Y. C. Chou, H. Zhao, L. Chen, X. Ma, and J. Liu, "Network characteristics of LEO satellite constellations: A Starlink-based measurement from end users," in *IEEE INFOCOM 2023-IEEE Conference on Computer Communications*, pp. 1–10, IEEE, 2023.
- [54] J. Pan, J. Zhao, and L. Cai, "Measuring a low-earth-orbit satellite network," 2023.
- [55] T. Kelso, "CelesTrak: Current NORAD two-line element sets." <https://www.celestrak.com/NORAD/elements/>, 2024.
- [56] S. Insider, "Starlink ground station locations: An overview." <https://starlinkinsider.com/starlink-gateway-locations>, 2024. Online.
- [57] S.-T. Team, "Space-track." <https://www.space-track.org/>, 2024. Online.
- [58] J. Zhao and J. Pan, "LENS: A LEO satellite network measurement dataset," in *Proceedings of the 15th ACM Multimedia Systems Conference*, pp. 278–284, 2024.
- [59] RIPE, "RIPE Atlas." <https://atlas.ripe.net/>, 2024.
- [60] MaxMind, "GeoIP accuracy comparison." <https://www.maxmind.com/en/geoip-accuracy-comparison>, 2024.
- [61] M. Maltsev, "Stem." <https://github.com/torproject/stem>, 2023.
- [62] A. Johnson, C. Wacek, R. Jansen, M. Sherr, and P. Syverson, "Users get routed: Traffic correlation on Tor by realistic adversaries," in *Proceedings of the 20th ACM Conference on Computer and Communications Security*, 2013.
- [63] T. Elahi, K. Bauer, M. AlSabah, R. Dingledine, and I. Goldberg, "Changing of the guards: A framework for understanding and improving entry guard selection in Tor," in *Proceedings of the 2012 ACM Workshop on Privacy in the Electronic Society*, pp. 43–54, 2012.
- [64] J. Y. Yen, "Finding the k shortest loopless paths in a network," *management Science*, vol. 17, no. 11, pp. 712–716, 1971.
- [65] L. Izhikevich, M. Tran, K. Izhikevich, G. Akiwate, and Z. Durumeric, "Democratizing LEO satellite network measurement," *Proceedings of the ACM on Measurement and Analysis of Computing Systems*, vol. 8, no. 1, pp. 1–26, 2024.
- [66] K. Linux, "hping3." <https://www.kali.org/tools/hping3/>, 2024.
- [67] P. Kampanakis and W. Childs-Klein, "The impact of data-heavy, post-quantum TLS 1.3 on the time-to-last-byte of real-world connections," in *Workshop on Measurements, Attacks, and Defenses for the Web (MADWeb)*, 2024.
- [68] Medium, "Statistics behind latency metrics: Understanding p90, p95, and p99." <https://medium.com/tuanhdotnet/statistics-behind-latency-metrics-understanding-p90-p95-and-p99-dc87420d505d>, 2024. Online.
- [69] IPinfo, "IPinfo: Trusted IP data provider." <https://ipinfo.io/>, 2024.
- [70] CableTV, "Best fiber internet providers: Prices, speeds, and more." <https://www.cabletv.com/internet/best-fiber-internet-providers/>, 2025. Online.
- [71] T. T. Project, "Relay requirements." <https://community.torproject.org/relay/relays-requirements/>, 2024. Online.
- [72] C. Sendner, J. Stang, A. Dmitrienko, R. Wijewickrama, and M. Jadhwal, "MirageFlow: A new bandwidth inflation attack on Tor," in *Network and Distributed System Security (NDSS) Symposium*, 2024.
- [73] N. Mathews, J. K. Holland, S. E. Oh, M. S. Rahman, N. Hopper, and M. Wright, "Sok: A critical evaluation of efficient website fingerprinting defenses," in *2023 IEEE Symposium on Security and Privacy (SP)*, pp. 969–986, IEEE, 2023.
- [74] S. E. Oh, T. Yang, N. Mathews, J. K. Holland, M. S. Rahman, N. Hopper, and M. Wright, "DeepCoFFEA: Improved flow correlation attacks on Tor via metric learning and amplification," in *2022 IEEE Symposium on Security and Privacy (SP)*, pp. 1915–1932, IEEE, 2022.

- [75] Y. Sun, A. Edmundson, L. Vanbever, O. Li, J. Rexford, M. Chiang, and P. Mittal, “RAPTOR: Routing attacks on privacy in Tor,” in *24th USENIX Security Symposium (USENIX Security 15)*, pp. 271–286, 2015.
- [76] Y. Sun, A. Edmundson, N. Feamster, M. Chiang, and P. Mittal, “Counter-RAPTOR: Safeguarding Tor against active routing attacks,” in *2017 IEEE Symposium on Security and Privacy (SP)*, pp. 977–992, IEEE, 2017.
- [77] A. Master and C. Garman, “A worldwide view of nation-state Internet censorship,” *Free and Open Communications on the Internet*, 2023.
- [78] Amazon, “Project Kuiper.” <https://www.aboutamazon.com/what-we-do/devices-services/project-kuiper/>, 2025. Online.
- [79] P. Singh, D. Barradas, T. Elahi, and N. Limam, “Connecting the dots in the sky: Website fingerprinting in low earth orbit satellite Internet,” *Network and Distributed System Security Symposium (NDSS)*, 2024.
- [80] R. Fanou, F. Valera, and A. Dhamdhere, “Investigating the causes of congestion on the African IXP substrate,” in *Proceedings of the 2017 Internet Measurement Conference*, pp. 57–63, 2017.
- [81] I. Livadariu, A. Elmokashfi, and A. Dhamdhere, “Characterizing IPv6 control and data plane stability,” in *IEEE INFOCOM 2016-The 35th Annual IEEE International Conference on Computer Communications*, pp. 1–9, IEEE, 2016.
- [82] R. Fontugne, A. Shah, and K. Cho, “Persistent last-mile congestion: Not so uncommon,” in *Proceedings of the ACM internet measurement conference*, pp. 420–427, 2020.
- [83] M. Luckie, A. Dhamdhere, D. Clark, B. Huffaker, and K. Claffy, “Challenges in inferring Internet interdomain congestion,” in *Proceedings of the 2014 Conference on Internet Measurement Conference*, pp. 15–22, 2014.
- [84] A. Dhamdhere, D. D. Clark, A. Gamero-Garrido, M. Luckie, R. K. Mok, G. Akiwate, K. Gogia, V. Bajpai, A. C. Snoeren, and K. Claffy, “Inferring persistent interdomain congestion,” in *Proceedings of the 2018 Conference of the ACM Special Interest Group on Data Communication*, pp. 1–15, 2018.
- [85] M. Nasr, A. Bahramali, and A. Houmansadr, “DeepCorr: Strong flow correlation attacks on Tor using deep learning,” in *Proceedings of the 2018 ACM SIGSAC Conference on Computer and Communications Security*, pp. 1962–1976, 2018.
- [86] F. Rochet and O. Pereira, “Dropping on the edge: Flexibility and traffic confirmation in onion routing protocols,” *Proceedings on Privacy Enhancing Technology*, vol. 2018, no. 2, pp. 27–46, 2018.
- [87] L. Yang and F. Li, “mTor: A multipath Tor routing beyond bandwidth throttling,” in *2015 IEEE Conference on Communications and Network Security (CNS)*, pp. 479–487, IEEE, 2015.

Appendix

1. Physical Limit of Fiber Transmission

Fiber optic cables work on the principle of total internal reflection. A light signal (carrying information encoded in this form) is sent down the cable at an angle greater than the *critical angle* for the medium, and travels the length of the cable by being reflected back and forth between the two cladded walls of the cable. Only in a perfectly straight length of fiber cable may the light travel in a straight line, however, in practical settings where bends are inevitable the light travels by bouncing from wall to wall. Hence, the light often travels a longer distance than the length of the cable.

A typical value of the critical angle is 82° and the diameter of a single mode fibre (as used in long haul cables)

TABLE 3. BASELINE SATELLITE LATENCY FROM LENS DATASET

Dish Loc.	PoP Loc.	Route Len. (km)	Duration	Data Num.
Alaska	Seattle	5,119	26 days	134.81M
Frankfurt	Frankfurt	2,200	40 days	227.58M
Seattle	Seattle	2,200	46 days	264.89M
Seattle_hp	Seattle	2,200	54 days	327.21M
Vancouver	Seattle	2,234	59 days	333.94M
Victoria	Seattle	2,212	61 days	339.97M

TABLE 4. BASELINE TERRESTRIAL LATENCY FROM RIPE DATASET

Traffic Route Length (km)	Pairs Number	Data Number
0~2k	213,752	56.98M
2k~4k	55,388	13.23M
4k~6k	49,656	12.15M
6k~8k	96,827	22.28M
Total	415,623	104.64M

is 9 microns. This means that the light travels a roughly 1% longer distance as compared to the length of the fiber cable. For example, on a trip down a 1,000 km length of fiber cable, the light will travel 1,010 km. Note that transmission over a single fiber cable cannot be done over distance of greater than ≈ 100 km, requiring repeaters along the path.

2. Baseline Latency Measurement

Baseline Latency Dataset. Table 3 shows the satellite latency data collected from LENS dataset. The measurements were conducted across five geographical locations: Alaska, Frankfurt, Seattle, Vancouver, and Victoria. Seattle has two dishes subscribing to Starlink’s regular and high-priority service plan. We extract a total 1.624 billion data points of ICMP latencies from the LENS dataset, spanning a two-month period from April to May, 2024. As of terrestrial latency, as listed in Table 4, we extract over 104.64 million data points from RIPE dataset, covering a one-week period starting on Sep. 2, 2024. The data is divided based on the round-trip length, by a 2k kilometers interval.

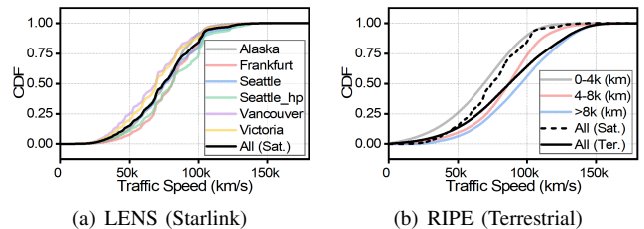


Figure 15. Traffic speed CDF of satellite link (measured in Starlink) and terrestrial link (RIPE Dataset).

Baseline Traffic Speed. The cumulative distribution function (CDF) for the speed of satellite and terrestrial traffic is derived from LENS and RIPE datasets. The latencies are measured using ICMP transmissions, capturing all practical latency components including transmission, congestion, and processing delays. They also capture any practical factors that affect satellite routing latencies, involving satellite movement, weather conditions, and network reconfiguration

[29]. Continuously sampling from this CDF over an extended duration can replicate the long-term latency characteristics of satellite and terrestrial routing at a global scale.

Fig. 15(a) presents the satellite traffic speed measured over Starlink across five locations. Seattle measurements include two dishes with regular and high-priority subscriptions, with the latter expected to show better latency performance. The round-trip length of satellite traffic $\approx 2,200$ km, except for the Alaska dish, which is around 5,119 km. The figure shows that the Vancouver dish (light purple curve) exhibits the slowest traffic speed, while the Frankfurt dish (light red) and the Seattle priority dish (light green) demonstrate the best speed performance. The Alaska dish, with a different round-trip length from all other dishes, presents a medium speed performance, implying that round-trip length of transmission has no impact on traffic speed. The traffic speed variations across global locations may result from the different density of the satellite constellation and ground stations, dish performance, and service plans. The combinatorial CDF across all locations (black curve) shows that satellite traffic transmits slower than 50k kilometers per second during $\approx 15\%$ of the time, and slower than 100k km/s during $\approx 85\%$ of the time.

The terrestrial traffic speeds are measured across more than 12,000 global probes on the RIPE Atlas platform. The distances between probe pairs range from 0.06 to 10k kilometers, corresponding to round-trip route lengths of 0.12 to 20k kilometers. Note that these figures are straight-line distances, disregarding the detours within actual routing paths through intermediate devices. Fig. 15(b) shows the terrestrial speed CDF grouped by round-trip length, indicating that shorter round-trip correspond to slower traffic transmission. The speed CDF for round-trip lengths between 0 and 4k kilometers, represented by the transparent black curve, is above all other curves, indicating that a larger portion of the data is concentrated within the lower speed range. In contrast, transmissions exceeding 8k kilometers, represented by the transparent blue curve, exhibit the fastest traffic speeds among all sub-groups. This is probably because long-distance transmissions, such as links between Europe and America, often utilize high-capacity backbone connections optimized for global communication, whereas shorter transmissions may experience slower speeds from local congestion or suboptimal inter-domain routing.

Another observation from Fig. 15(b) is that, in general, satellite traffic (black dashed curve) transmits faster than terrestrial traffic for round-trip distances between 0 and 4k kilometers. Beyond this range, satellite routing does not significantly outperform terrestrial routing in traffic speed but remains competitive, with a reasonable likelihood of being faster. However, higher transmission speed does not necessarily equate to lower latency, as the presented satellite speeds are calculated along longer physical paths that traverse one or more orbiting satellites, while terrestrial speeds are based on shorter, straight-line distances between ground-based measurement probes. Satellite routing is expected to yield lower latency only when its higher transmission speed offsets the longer path length—such as in cases involving

distant endpoints or congestion along terrestrial paths.

3. Satellite Routing Strategy

To determine the latency of a Tor circuit, it's necessary to estimate and then sum up the latency of each its individual hop. Estimating the satellite routing latency between two nodes requires an examination of possible routing strategies that may be adopted by satellite operator. This involves how the traffic is routed from the source through a sequence of satellites and ground stations to reach the destination. A graph model is used for evaluation, with each graph node representing an endpoint and each edge indicating a link.

3.1. Nodes in Satellite Routing Graph. Satellite routing involves four types of nodes. *User* means the sending and receiving party of satellite communication. In Tor, this could be a client, intermediate relay and destination server. *Satellite* circles the Earth at a fixed altitude. With current technology, satellites essentially act as a “mirror”, reflecting or forwarding signals without processing or caching. *Ground Station*, equipped with antennas and electronic transmitters, directly communicates with satellites for tracking, controlling and data relaying. *Point of Presence (PoP)* acts as a gateway between satellite and terrestrial networks. All traffic from satellite must pass through a ground station, and then a PoP before entering the terrestrial Internet.

3.2. Edges in Satellite Routing Graph. There are mainly six types of edges between the four types of nodes. *Inter-User Link (IUL)*, as shown by link 1 in Fig. 16(a), is the connection between users through terrestrial Internet. *User-Satellite Link (USL)*, which is the link 2 in the figure, transmits data from the sender to a nearby satellite. This link communicates using radio frequency(RF) beams through the Earth's atmosphere. *Inter-Satellite Link (ISL)*, as shown by link 3, is the laser-based connection between satellites that can transmit at the speed of light in a vacuum. This link is an imminent feature in certain satellite constellations such as SpaceX's Starlink, demonstrated by the evidence in Section 2. *Groundstation-Satellite Link (GSL)*, which is link 4, exchanges traffic between satellite and ground station using the RF beams, similar to USLs. *Groundstation-PoP link (GPL)*, which is link 5, transmits traffic from ground stations to PoPs before entering the terrestrial Internet. Each ground station is often paired with a nearby PoP, and the GPL latency ≈ 5 ms globally [29]. *User-PoP Link (UPL)*, as shown by link 6, exchanges traffic between PoPs and users. This link goes through the terrestrial Internet, and its speed depends on the quality of the local network service.

3.3. Possible Routing Strategies. By varying the availability of links, routing graphs with different connectivity can be constructed, corresponding to a range of routing strategies. Fig. 16(b) illustrates traditional terrestrial routing, where neither relay has access to satellite network, thus only IUL is available. Fig. 16(c) depicts the scenario where USL, GSL, GPL and UPL are available. Under this setting, traffic from

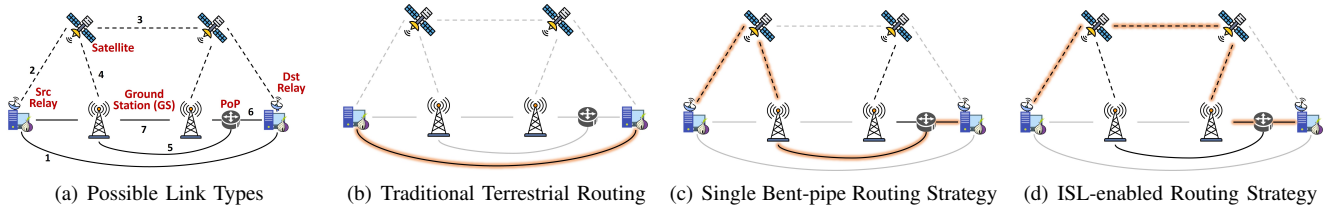


Figure 16. Routing graph between relays, where dash and solid line are space and ground link, respectively. Black line indicates valid links while gray means invalid ones. Different routing strategies are modeled by switching link availability.

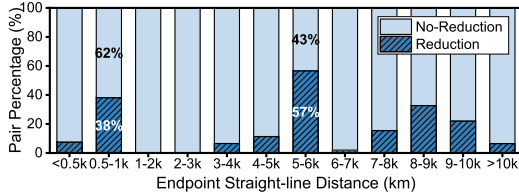


Figure 17. SaTor latency reduction efficacy across varying end-to-end distance between relay pairs.

the source relay could first travel to the satellite-1 and down to a nearby ground station, forming a “bent-pipe” structure. The ground station forwards the traffic to PoP, and then to destination through terrestrial network. This single bent-pipe routing is currently adopted in most satellite transmissions.

Assuming the availability of ISLs, routing graph would be like Fig. 16(d), where traffic originating from the source are relayed across multiple satellites before reaching a ground station near the destination. This “ISL-enabled” routing keeps traffic in space for most of its journey, thus effectively utilizing the acceleration potential of satellite transmission. By utilizing a shortest-path algorithm on different routing graphs, SaTor simulator can estimate latency for circuits across various routing strategies.

4. Satellite Routing across Varying Distance

Fig. 17 shows latency variation grouped by end-to-end geographic distance. Satellite routing achieves the most significant gains in the 500–1k km (38% of pairs) and 5–6k km (57%) ranges. Moderate improvements (20–40%) are also observed at 8–10k km. This section provides only an intuitive explanation of the relationship between geographic distance and latency reduction efficacy. A comprehensive analysis of other factors, such as satellite orbital characteristics, constellation orchestration, and the density of ground stations, remains an important topic for future work.

For connections shorter than 500 km, terrestrial routing is already fast, while the bent-pipe structure of satellite links adds propagation overhead. In the 0.5–1k km range, terrestrial delays are often inflated due to local congestion or inefficient routing across regional ASes. Between 1k and 3k km, terrestrial traffic might be handed off to Tier-1 backbones, enabling optimized routing to reduce AS-path inflation. The 5–6k km range often involves transoceanic links, where terrestrial routes may experience congestion during

suboptimal cable routing, while satellite paths with inter-satellite links can provide more stable and direct delivery. Beyond 6k km, the satellite advantage diminishes, possibly due to increased ISL hops and routing inefficiencies.

5. SaTor in the Real World

A key requirement of SaTor’s practical deployment is the availability of satellite services in the region where a relay is located. According to SpaceX’s website, Starlink services are currently offered in over 65 countries. As of December 2024, out of 8,730 Tor relays in total, 8,280 (94%) are situated in countries where Starlink is operational. Among the remaining 450 relays, 103 are in countries where Starlink is expected to become available soon, while 347 are in regions with no clear timeline for service introduction. These findings indicate that a majority of relays are located in areas where Starlink service is either already accessible or expected to launch in the near future, demonstrating the practicality of SaTor under current conditions.

Another factor affecting SaTor deployment is the type of network infrastructure hosting relays. Using data from Tor Metrics [1], we identified the Autonomous System (AS) for all relays and categorized them into four types based on the IPinfo database [69]: *cloud platform*, *general ISP*, *business network*, and *education network*. As Table 5 shows, cloud platforms are the most prevalent infrastructure, hosting 60% of the top 2k relays (ranked by bandwidth weight) and 70% of all 8,730 relays. Deploying SaTor on cloud-hosted relays is not a straightforward process, as it would require cloud provider to access their platform to satellite network. Fortunately, major cloud providers are moving in that direction. Cloud providers like Amazon, Google, and Microsoft are forging partnerships with satellite companies to enhance their service through satellite technology [35], [36]. This may facilitate SaTor deployment since satellite installation and management will be outsourced to the providers.

About 30% of relays are hosted on general ISP, business, or education networks. General ISPs may include residential networks or small institutions without their own ASs. SaTor deployment could be more straightforward on relays hosted in these infrastructures, as operators are likely to have direct access to physical machines for installing satellite equipment. Among the top 2k relays, 40% are hosted on non-cloud infrastructures—a sufficient number to realize SaTor’s potential. These relays have made substantial contributions to Tor’s bandwidth, reflecting a strong commitment to the

TABLE 5. AS TYPE OF TOR RELAYS

AS Type	Top-2k	Top-4k	Top-6k	All (8,730)
Cloud Plat.	1,199 (60%)	2,886 (72%)	4,393 (73%)	6,149 (70%)
General ISP	422 (21%)	571 (14%)	887 (15%)	1,771 (20%)
Business	66 (3%)	97 (2%)	233 (4%)	249 (3%)
Education	313 (16%)	445 (12%)	485 (8%)	559 (7%)

community. Given this, it is reasonable to expect that these operators would be open to adopting new technologies aimed at enhancing the network's performance.